Supplementary Material (ESI) for Dalton Transactions

Supporting Information

Functions of $LiBH_4$ in the hydrogen sorption reactions of 2LiH-$Mg(NH_2)_2$ system

Jianjiang Hu[1], Eveline Weidner[2], M. Hoelzel[3] and Maximilian Fichtner[1]

[1]Institute of Nanotechnology, Karlsruhe Institute of Technology, P.O. Box 3640, D-76021 Karlsruhe, Germany
[2]JRC Institute for Energy, Cleaner Energy Unit, Petten, the Netherlands
[3]Forschungs-Neutronequelle Heinz Maier-Leibnitz, Lichtenbergstrasse 1, 85747, Garching, Germany

Kissinger Plots for $Mg(NH_2)_2$-2LiH-0.3$LiBH_4$ and $Mg(NH_2)_2$-2LiH-0.67$LiBH_4$

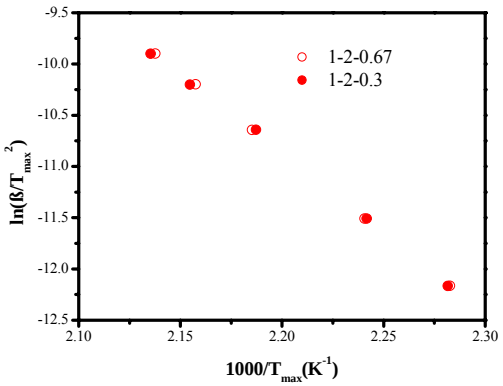

Figure S1 Kissinger Plots for $Mg(NH_2)_2$-2LiH-0.3$LiBH_4$ and $Mg(NH_2)_2$-2LiH-0.67$LiBH_4$

Determination of transient activation energy

To determine the transient activation energy using the method described in the manuscript, dehydrogenation was performed at ramping rates β_1 = 2 °C/min and β_2 = 5 °C/min, respectively. In the time - conversion (t - α) (Figure S2) and temperature - conversion (T – α) (Figure S3) plots, the transient times (t_{1i} and t_{2i}) and temperature (T_{1i} and T_{2i}) at conversion α_i can be obtained via equations (1) and (2), corresponding to ramping rates β_1 and β_2, respectively. The transient Ea can be calculated through equation (3).

$$t_{lik} = \frac{t_{li} + t_{lk}}{2} (l = 1,2) \qquad (1)$$

$$T_{lik} = \frac{T_{li} + T_{lk}}{2} (l = 1,2) \qquad (2)$$

$$E_a = R \frac{T_{1ik} T_{2ik}}{T_{2ik} - T_{1ik}} \ln \frac{\Delta t_1}{\Delta t_2} \qquad (3)$$

Where t_{1i} and t_{1k} are times at the conversion degrees α_i and α_k for the heating rate β_1; T_{1i} and T_{1k} are the temperatures at the conversion degrees α_i and α_k for the heating rate β_1. t_{2i} and t_{2k} are times at the conversion degrees α_i and α_k for the heating rate β_2; T_{2i} and T_{2k} are the temperatures at the conversion degrees α_i and α_k for the heating rate β_2 ($\beta_2 > \beta_1$). The calculated activation energy from equation (3) corresponds to the conversion at

$$\alpha = \frac{\alpha_i + \alpha_k}{2} \qquad (4).$$

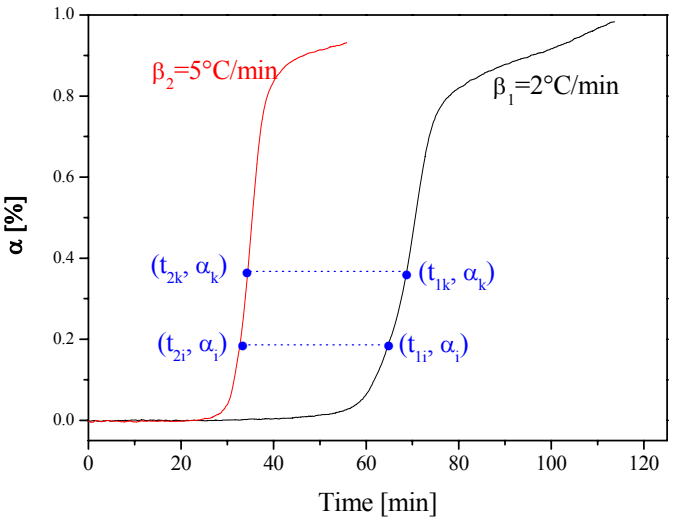

Figure S2 Conversion as a function of time at heating rates of β_1 = 2 °C/min and β_2 = 5 °C/min

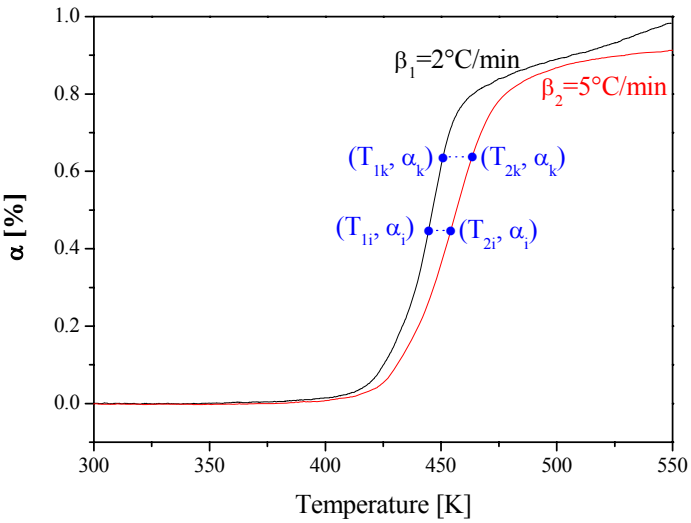

Figure S3 Conversion as a function of temperature at heating rates of β_1 = 2 °C/min and β_2 = 5 °C/min

Estimation of crystallinity of $Mg(NH_2)_2$ in $LiBH_4$ doped samples

Figure S4 shows the crystallization heat effect of $Mg(NH_2)_2$ measured by DSC. Since the content of magnesium amide in the sample $Mg(NH_2)_2$-2LiH-0.3$LiBH_4$ is 71.2 %, the crystallinity in this sample was estimated via the fraction of heat effect originated from the sample (-45.91 J/g as shown in Figure S4) divided by the crystallization enthalpy of $Mg(NH_2)_2$ (-140.0 J/g):

$$45.91/140/71.2\% = 46.1\%$$

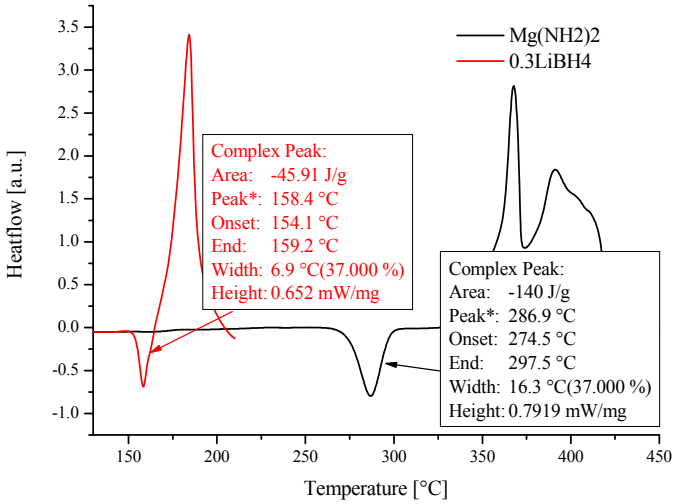

Figure S4 Crystallization enthalpies measured by DSC for pure $Mg(NH_2)_2$ and mixture $Mg(NH_2)_2$-2LiH-0.3$LiBH_4$

Crystallization of $Mg(NH_2)_2$ from amorphous state

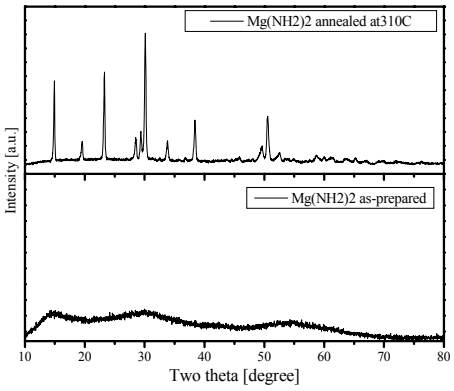

Fig. S5 XRD profiles of $Mg(NH_2)_2$: as-prepared by ball milling MgH_2 with NH_3 (lower) and annealed at 310°C

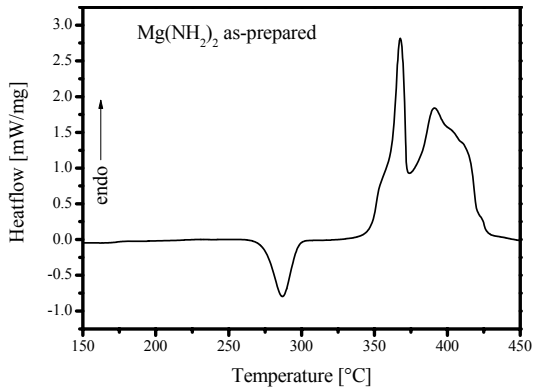

Fig. S6 DSC curve of as-prepared $Mg(NH_2)_2$

FTIR spectra at various desorption stages

Figures S7 and S8 are the FTIR spectra for samples $Mg(NH_2)_2$-2LiH-0.3$LiBH_4$ and $Mg(NH_2)_2$-2LiH-0.67$LiBH_4$, respectively. It can be seen that the strong absorbance attributed to B-H stretching in the range 2100 – 2400 cm^{-1} was not affected by different hydrogen desorption extent.

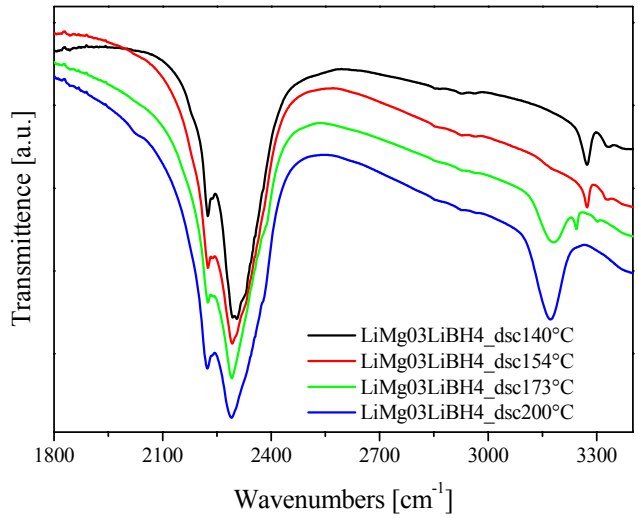

Figure S7 FTIR spectra of $Mg(NH_2)_2$-2LiH-0.3$LiBH_4$ heated to 140°, 154°, 173° and 200 °C

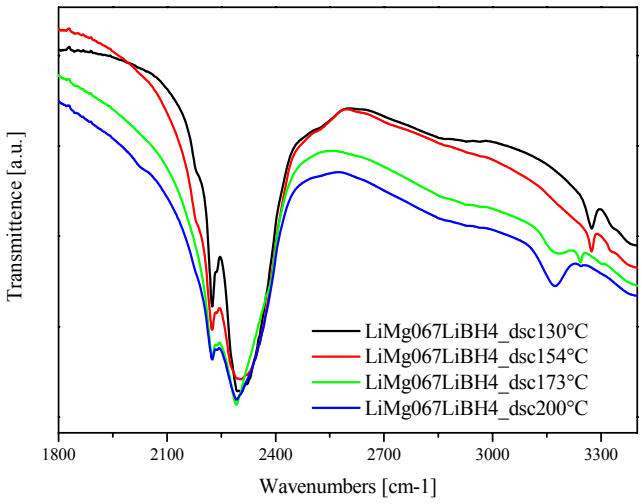

Figure S8 FTIR spectra of $Mg(NH_2)_2$-2LiH-0.67$LiBH_4$ heated to 130 °, 154 °, 173 ° and 200 °C

Preparation of $Li_4(^{11}BD_4)(NH_2)_3$ with high crystallinity

$Li_4(^{11}BD_4)(NH_2)_3$ melts at about 220 °C, as shown in Figure S9 (red curve). In order to obtain $Li_4(^{11}BD_4)(NH_2)_3$ with high crystallinity, the ball milled mixture of $Li^{11}BD_4$ with $LiNH_2$ at 1:3 molar ratio was heated to 230 °C (just above its melting point) and kept at the temperature for 1 h, then cooled down slowly to room temperature. Figure S10 shows the strong diffraction intensity of annealed $Li_4(^{11}BD_4)(NH_2)_3$, compared to the as-milled product.

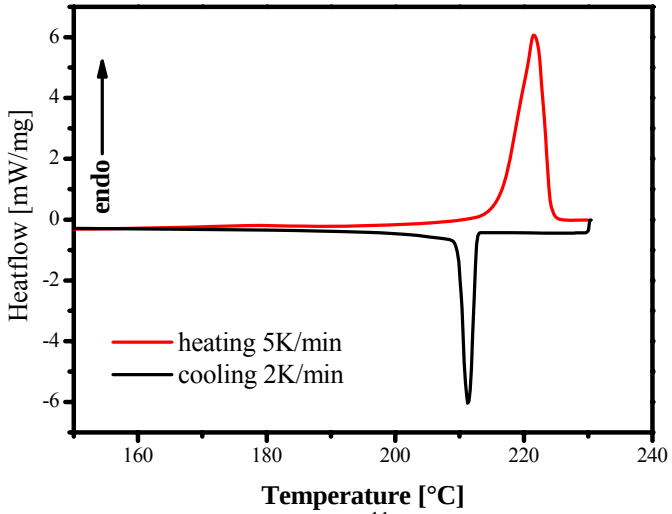

Figure S9 DSC curves of $Li_4(^{11}BD_4)(NH_2)_3$ from milled mixture of $Li^{11}BD_4$ with $LiNH_2$ at 1:3 molar ratio.

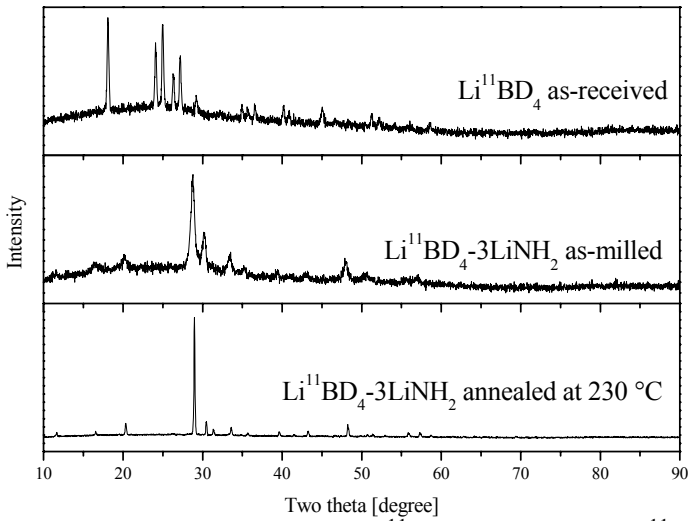

Figure S10 XRD patterns of $Li^{11}BD_4$, as-milled $Li_4(^{11}BD_4)(NH_2)_3$ and annealed $Li_4(^{11}BD_4)(NH_2)_3$.